Experimental Evaluation of Test Methods to Characterize Tensile Behavior of Ultra-High Performance Concrete

Authors & Affiliation:

Daniel Bridi Valentim – Ph.D. student, 2024 South Engineering Research Center, Department of Civil, Construction, and Environmental Engineering, University of Alabama, Tuscaloosa, AL 35487 USA, Phone: 205-393-3785, Email: dbridivalentim@crimson.ua.edu

Sriram Aaleti, Ph.D.* (corresponding author) – Assistant Professor, 2037-C South Engineering Research Center, Department of Civil, Construction, and Environmental Engineering, University of Alabama, Tuscaloosa, AL 35487 USA, Phone: 205-348-5110, Email: saaleti@eng.ua.edu

Armen Amirkhanian, Ph.D., P.E. – Assistant Professor, 2013-G South Engineering Research Center, Department of Civil, Construction, and Environmental Engineering, University of Alabama, Tuscaloosa, AL 35487 USA, Phone: 205-348-0785, Email: armen.amirkhanian@eng.ua.edu

Michael E. Kreger, Ph.D., P.E. – Garry Neil Drummond Endowed Chair in Civil Engineering, 2037-G South Engineering Research Center, Department of Civil, Construction, and Environmental Engineering, University of Alabama, Tuscaloosa, AL 35487 USA, Phone: 205-348-3213, Email: mekreger@eng.ua.edu

Abstract:

Ultra-high performance concrete (UHPC) is a relatively new class of concrete material that exhibits exceptional mechanical and durability properties compared to traditional concrete. Unlike normal concrete, UHPC has a sustained post-cracking tensile strength due to the presence of steel fibers and strain hardening of the fibers. The tensile response of UHPC plays an important role in the design of structural members. However, currently there is no standard test method available to reliably characterize the tensile behavior of UHPC. There are several experimental methods available in literature to quantify the tension behavior of steel fiber-reinforced concrete. The test methods include the disk-shaped compact tension (DCT) test, double-edge wedge-splitting (DEWS) test, single-edge notched beam specimen (SEN(B)), and four-point beam bending test. FHWA is currently developing a direct-tension test procedure for quantifying UHPC tension behavior. A total of 47 specimens, including at least 6 specimens for each type of test, were constructed using a commercially available UHPC mix and were tested to failure using standard test procedures. Using experimentally measured force-displacement response, fracture parameters and tensile stresses were calculated for different test methods. This paper presents details of the experimental investigation, observations, and observed correlation between the tension behavior obtained from the conducted tests.

Keywords: Ultra-High Performance Concrete, tensile strength, experimental methods

1. Introduction

Ultra-high performance concrete (UHPC) is a reactive powder concrete mixture. Combined with high-strength steel fibers, this relatively new class of concrete exhibits exceptional high compressive strength and durability compared to traditional concrete. Due to these exceptional properties, it is gaining interest among several departments of Transportation (DOTs) for construction and reconstruction of bridges and other critical highway structures (Graybeal, UHPC Making Strides). Unlike normal concrete, the presence of steel fibers gives UHPC a sustained post-cracking tensile strength resulting from strain hardening of the fibers. Moreover, while normal concrete typically has a compressive strength lower than 8 ksi, UHPC offers a compressive strength of at least 21.7 ksi (150 MPa) according to the Federal Highway Administration (FHWA) (Graybeal, Ultra-High Performance Concrete).

The first research work related to UHPC originated in the 1970s in Europe, and it was recognized as a potential new revolutionary material by the early 1990s (Perry). Nonetheless, it first became commercially available in the United States in the early 2000s. Since then, a series of research and real-word construction projects have been developed demonstrating the capabilities and potential uses of this material in bridges (Graybeal, Ultra-High Performance Concrete). The primary reason for major interest in usage of UHPC in bridges has been due to its sustained tensile strength, high durability, and high bond strength (small rebar development lengths). Due to the fact that it is a relatively new material in the research community and construction industry, there is a need for standardized test methods for assessing its mechanical properties.

When compared with normal concrete, the tensile response of UHPC is a feature that stands out and can play a significant role in design of structural members. Several researchers have used existing test methods for fiber-reinforced concrete (FRC) or traditional concrete to quantify UHPC's tensile strength. However, there is still a lack of a standard test method for characterizing tensile behavior of UHPC and correlation among different test methods. This paper presents details of the experimental investigation involving several existing test methods, observations, and observed correlation between the tension capacities obtained from the conducted test methods. The test methods investigated in this study include the disk-shaped compact tension (DCT) test (Amirkhanian et al.), double-edge wedge-splitting (DEWS) test (di Prisco et al.), single-edge notched beam specimen (SEN(B)) (RILEM TC 89-FMT), four-point bending test, and direct-tension test (Graybeal and Baby, Development of Direct Tension Test Method for Ultra-High-Performance Fiber-Reinforced Concrete).

2. Background

The applications for UHPC have been constantly increasing as its mechanical and durability properties have been studied and better understood. This exceptional cementitious material can be used in different types of structural and architectural elements such as bridge girders, bridge decks, pile foundations, earthquake-resistant columns, wind turbine towers, bridge connections (Sritharan), and building facades (Lorenzo et al.). As use of UHPC material increases, so does the need for the standardization of estimating its properties. Accurately establishing the mechanical properties of UHPC reduces the variation of the material coefficients and helps designers implement a more reliable and economical design.

Currently, ASTM C1856/1856M establishes a standard testing method for obtaining the compressive strength of UHPC using standard 3 by 6-in. cylinders, and refers to ASTM 1609/C1609M standard test method to determine the flexural strength of UHPC beams subjected

to a third-point loading (four-point bending) test. In the study presented in this paper, we present two other types of UHPC geometries, namely, DCT and DEWS. These geometries can be easily cored from already existing structures and might provide a better option for estimating in-situ strength of UHPC. The DCT specimen can be cored using a 6-in. (15.24-cm) hole saw on an existing structure or can be cast in the laboratory/field using standard 6-in. (15.24-cm) diameter cylinder molds. The DEWS specimen can also be cored as a rectangular prism with a squared cross section and finished with concrete or tile saw afterwards. Moreover, unlike the DCT or direct tensile test method, the DEWS geometry has the advantage that its test setup requires a compression machine instead of tension-based equipment, which could significantly improve the availability of testing facilities and ease of testing. A more widely studied geometry in fiber reinforced concrete, the SEN(B), was also used in the experimental study to compare the critical crack tip opening displacement ($CTOD_c$) and the critical stress intensity factor (K_{IC}) with the DCT geometry. The stress intensity factor is a geometric-independent property that characterizes a material's resistance to fracture, and the critical stress intensity factor is the stress needed to initiate a crack in the material. Besides these three specimen types, direct tension rectangular beams and four-point bending beam specimens were also evaluated in this study.

3. Testing Methods and Experimental Testing

3.1. Specimen Fabrication

All specimens were fabricated with the aim of geometric perfection so that the experimental data would not be affected by shape defects. A computer numerical control (CNC) machine was used to ensure the control specimen dimensions which had a more delicate and irregular geometry. Figure 1 (a) and Figure 1 (b) show the formwork geometries for the DEWS and DCT test specimens, respectively. The wooden formwork was secured on an acrylic base to make the bottom of the specimen completely flat and smooth. Despite the fact that wood was the main material used in the specimen formwork fabrication all wooden formwork parts in contact with UHPC were waterproofed using a sprayable rubber coating (see Figure 1 (c)), preventing the wood from absorbing any water from the UHPC mix, which may affect hydration and material properties. For the case of rectangular beam and direct tensile test specimens, formwork in contact with UHPC was covered with a plastic waterproof adhesive layer, as shown in Figure 1 (d).

3.2. Casting and curing

The UHPC mix design (Table 1) used in this experimental investigation was composed of a premix (Ductal® JS1000) provided by Lafarge®, superplasticizer (Premia 150), and steel fibers (2% by volume). A standard Mortarman® high shear horizontal mixer (see Figure 1(e)) was used for the UHPC mixing process, ensuring an even distribution of steel fibers. All test specimens for the different test methods were cast on the same day. As shown in Figure 1 (f), the UHPC mix was poured from one side for all of the specimens, letting UHPC freely flow and allowing a preferential orientation of fibers along the specimen length (i.e., perpendicular to crack propagation). After casting, all specimens were covered with a plastic sheet to minimize water evaporation. Approximately 24 hours after casting, all specimens were moved to an environmental chamber at 104°F (40°C) and 95% humidity, and cured for 72 hours. This was done to accelerate strength gain. Specimens were constantly wetted by being covered with wet burlap to minimize any possible shrinkage cracks.

Table 1. UHPC Mix Design used for casting test specimens

Material	lb/yd^3 (kg/m^3)
Premix	3699 (2194)
Water	219 (130)
Premia 150	51 (30)
Steel fibers (2% by volume)	263 (156)

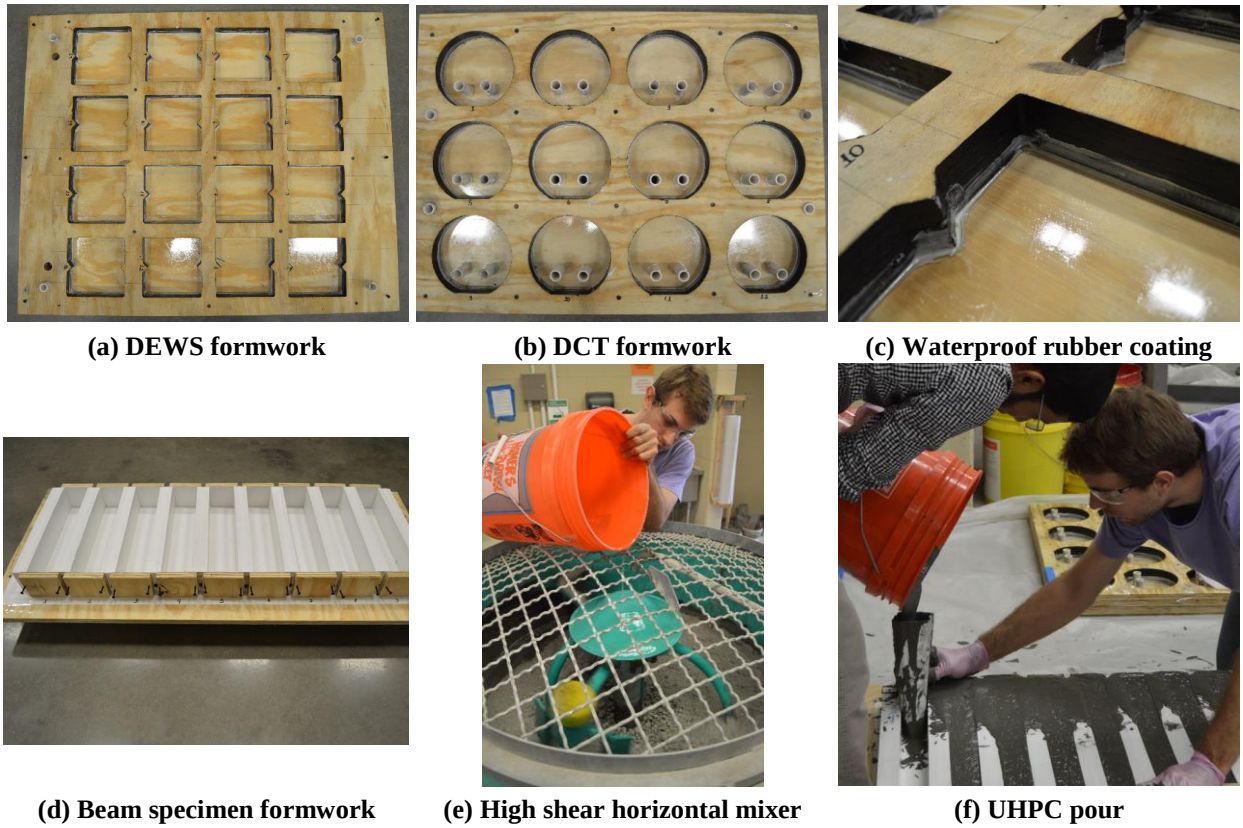

(a) DEWS formwork **(b) DCT formwork** **(c) Waterproof rubber coating**

(d) Beam specimen formwork **(e) High shear horizontal mixer** **(f) UHPC pour**

Figure 1. Specimen formwork and mixing, casting of UHPC

3.3. Testing procedures

All tests in this study were performed at room temperature using closed-loop servo-hydraulic MTS testing frames. The compressive strength of UHPC at the time of testing varied between 24.8 ksi (171 MPa) to 28.3 ksi (195 MPa).

3.3.1. Disk-shaped Compact Tension (DCT) Test

The DCT test specimen geometry was adopted from Amirkhanian et al. The thickness of the specimen was reduced from 2 in. (5.08 cm) to 1.5 in. (3.81 cm) in order to facilitate the production of the formwork built by a computer numerical control (CNC) machine. In addition, due to the absence of coarse aggregate in UHPC, the thickness of the specimen could be further reduced with the limiting factor being the steel fiber length. Geometry of the DCT specimen is illustrated in Figure 2, and dimensions are summarized in Table 2.

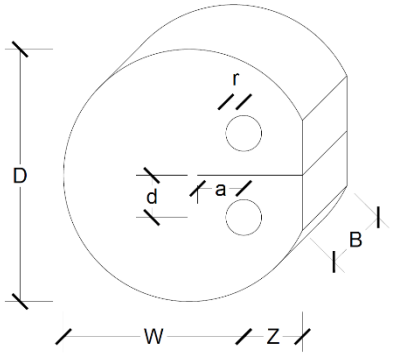

Figure 2. DCT Geometry

Table 2. DCT specimen geometry details

Dimension	Value, in. (cm)
D	6 (15.24)
W	4.3 (10.92)
Z	1.4 (3.56)
d	1 (2.54)
a	1.1 (2.79)
r	0.43 (1.09)
B	1.5 (3.81)
n (saw-blade thickness)	0.05 (0.13)
h (knife-edge thickness)	0.02 (0.05)

Tensile loading to the DCT specimen was applied using steel rods placed through the circular holes on each side of the pre crack. The test was performed under displacement control at a rate of 7.87 x 10^{-5} in/s (0.002 mm/s). When the load on the specimen reached 90% of the maximum force beyond its peak, the load was reduced at the same rate as used to load the specimen. As soon as the measured load dropped to 5% of the measured peak load, the specimen was reloaded at a rate of 3.94 x 10^{-4} in/s (0.01 mm/s). This load-unload cycle was necessary to obtain the loading and unloading compliances of the material. A standard clip gauge was used to record the crack mouth opening displacement (CMOD) of the specimen. The results obtained by the force and CMOD of each specimen were used to calculate its fracture properties according to the procedure described in Amirkhanian et al. The crack length ratio (α) corrects for the gauge point thickness (h), and it is given by Equation 1. With the crack length ratio known, the K_{IC} geometric correction factor, $F(\alpha)$, derived from numerical analysis, is calculated using Equation 2. Finally, it is possible to calculate the critical stress intensity factor (K_{IC}) and the critical crack-tip opening displacement ($CTOD_c$), using Equation 3 and Equation 5, respectively.

$$\alpha = \frac{a+h}{W+h} \quad (1)$$

$$F(\alpha) = \frac{-1.498\alpha^3 + 4.569\alpha^2 - 1.078\alpha + 0.113}{\alpha^4 - 2.408\alpha^3 + 1.717\alpha^2 - 0.3467\alpha + 0.0348} \quad (2)$$

$$K_{IC} = \sigma\sqrt{W}F(\alpha_{critical}) \quad (3)$$

$$\sigma = \frac{P}{WB} \quad (4)$$

$$CTOD_c = \frac{2\sigma W V_{CTOD}(\alpha_{critical})}{E} \quad (5)$$

where σ is the nominal stress at peak load, and P is the peak load. The elastic modulus, E, and $V_{CTOD}(\alpha_{critical})$ are calculated according to Amirkhanian et al.

3.3.2. Double-edge wedge-splitting (DEWS) Test

A preliminary geometry suggested by di Prisco et al. was slightly modified and used in this study. Figure 3 shows the specimen geometry. Two 0.75-in. (19.05-mm) diameter steel rollers placed in the 45 degree triangular grooves were used to compress the DEWS specimens. Metal assembly paste was used in the interface between the specimens and rollers to minimize friction as much as possible, making friction between the rollers and specimen close to zero and the vertical force applied equal to the horizontal resultant force. Based on this assumption the DEWS test results could be directly compared with the direct tension beam tensile strength.

The test was performed under displacement control, starting with a rate of 0.051 in/s (1.295 mm/s) until a 0.078-in. (2-mm) displacement was reached, which occurred after the peak load. Subsequently, the loading rate was increased to 0.102 in/s (0.004 mm/s) up to 0.157 in. (4 mm), which represents an approximately 80% drop in the peak load. Finally, the displacement rate was increased to 0.203 in/s (0.008 mm/s) until the specimen was split into two parts.

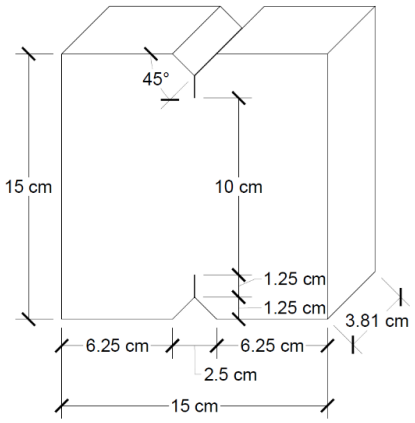

Figure 3. DEWS geometry

3.3.3. Single-edge notched beam (SEN(B)) Test

The SEN(B) specimens were 3 in. (7.62 cm) by 3 in. (7.62 cm) in cross-section and 14 in. (35.56 cm) long. After the specimens were cast and thermally cured, a notch of 0.75 in. (1.91 cm) (one fourth of the beam height) was made at the center of each beam. The specimens were simply supported over a 12-in. (30.48-cm) span, and a point load was applied at the center of the beam (at the notch center line). Load was applied under displacement control at a rate of 1.969 x 10^{-4} in/s (0.005 mm/s). At 95% of the maximum applied force past peak load, the specimen was unloaded at a rate of 1.969 x 10^{-3} in/s (0.05 mm/s) until the recorded force reached zero. The specimen was then reloaded at the same unloading rate. In order to capture the CMOD of each specimen, a clip gauge was used and placed at the bottom of the specimen at the tip of the notch. Similar to the DCT test, this load-unload cycle was necessary to obtain the loading and unloading compliances of the material. Based on the specimen geometry, the load applied, and the CMOD readings, fracture parameters for each specimen were calculated according to RILEM TC 89-FTM. The geometric correction factor, $F(\alpha)$, was calculated using Equation 6. The critical stress intensity factor (K_{IC}) and the critical crack tip opening displacement ($CTOD_c$) were obtained by Equation 7 and Equation 8.

$$F(\alpha) = \frac{1}{\sqrt{\pi}} \frac{1.99 - \alpha(1-\alpha)(2.15 - 3.93\alpha + 2.7\alpha^2)}{(1+2\alpha)(1-\alpha)^{3/2}} \tag{6}$$

$$K_{IC} = 3(P_{max} + 0.5W) \frac{S(\pi a_c)^{1/2} F(\alpha)}{2d^2 b} \tag{7}$$

where α is the crack length ratio, P_{max} is the peak load, W is the self-weight of the specimen, S is the beam span (12 in. (30.48 cm)), a_c is the critical effective crack length, d is the height of the specimen (3 in. (7.62 cm)), and b is the specimen thickness (3 in. (7.62 cm)).

$$CTOD_c = \frac{6P_{max} S a_c V_1(\alpha)}{E d^2 b} [(1-\beta)^2 + (1.081 - 1.149\alpha)(\beta - \beta^2)]^{1/2} \tag{8}$$

Where, $\alpha = a_c/d$, and $\beta = a_{inital}/a_c$.

3.3.4. Four-point bending beams (4PB)

The four-point bending beam specimens had the same dimensions as the SEN(B) specimens. Similar to the SEN(B) specimens, the four-point bending beams (4PB) were also simply supported over a span of 12 in. (30.48 cm). The load was applied simultaneously at the two points that divide the span into 4-in. (10.16-cm) thirds. The specimens were loaded under displacement control at a loading rate of 5.906 x 10^{-4} in/s (0.015 mm/s) until failure. The peak strength was calculated using the formula for modulus of rupture according to ASTM C1609/C1609M (Equation 9).

$$f = \frac{PL}{bd^2} \tag{9}$$

where f is the strength, P is the load, L is the span length, b is the average width of the specimen at the fracture, and d is the average depth of the specimen at the fracture.

3.3.5. Direct tension beams

The direct tension beam specimens had a 2-in. (5.08-cm) square cross section, and length of 17 in. (43.18 cm). Aluminum plates were attached at the specimen ends to minimize stress concentrations while the beams were being gripped by the standard MTS tension testing equipment. The specimens were tested at a constant displacement control rate of 1 x 10^{-4} in/s (5.43 x 10^{-3} mm/s).

4. Results

To better visualize and understand the behavior and failure of each type of test, Figure 4 shows each specimen type immediately after failure. In the figure below, it is possible to observe the crack start location and the crack propagation direction. The experimental fracture parameters, obtained from the DCT and SEN(B) specimens, are summarized in Table 3 and Table 4, respectively. As previously explained, the tensile strength of the DEWS specimens was compared with results of the uni-axial tension test performed on the direct tension beams. Table 5 and Table 6 show the results calculated from the experimental data. Table 7 shows the flexural stress of the four-point bending beams calculated based on the peak load of each specimen.

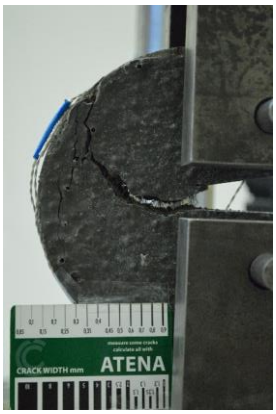

(a) DCT

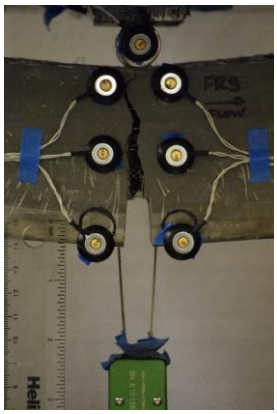

(b) SEN(B)

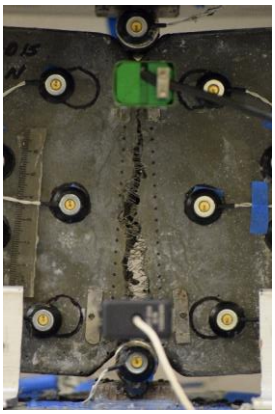

(c) DEWS

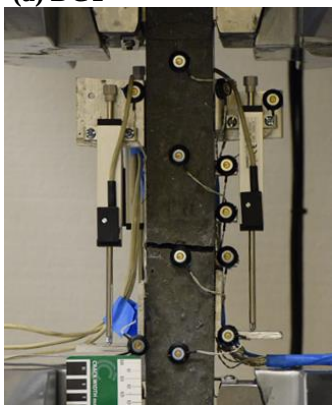

(d) Direct tension beam

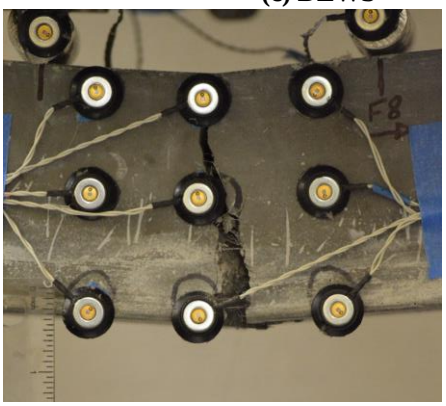

(e) Four-point bending beam

Figure 4. Observed failures of test specimens for different test methods

5. Discussion

As expected, the calculated critical stress intensity factors (K_{IC}) calculated for the SEN(B) and DCT specimens are higher than those for normal concrete (typically between 1 and 2 MPa · $m^{1/2}$ according to the results obtained by Amirkhanian et al.), since UHPC is a stiffer material and contains a significant amount of steel fibers. Using the geometric correction factor, $F(\alpha)$, adequate for each geometry, the K_{IC} calculated for the DCT and SEN(B) specimens have averages of 6.61 ksi · $in^{1/2}$ (7.26 MPa · $m^{1/2}$) and 6.40 ksi · $in^{1/2}$ (7.03 MPa · $m^{1/2}$), respectively. The $CTOD_c$ values for the DCT and SEN(B) specimens are 0.0075 in. (0.1894 mm) and 0.0076 in. (0.1930 mm). Both averages for K_{IC} and $CTOD_c$ were found to be statistically identical with a 95% confidence interval for a two-sample t-test.

All DCT specimens experienced the same failure pattern. While the initial crack formed at the notch across the width, crack propagation was quickly altered due to the presence of fiber reinforcement. However, the calculated K_{IC} and $CTOD_c$ values are only dependent on peak load behavior and thus the continued crack propagation, regardless of direction, had no impact on the analysis. With regard to the SEN(B) specimens, all failures occurred in the fracture ligament, at the applied concentrated load. For both the DCT and SEN(B), the fracture properties can be used to calculate the tensile strength of the material through modeling using the two-parameter fracture model by Jenq and Shah.

Table 3. DCT fracture parameters

Specimen	Force kip (kN)	σ ksi (MPa)	$CTOD_c$ in (mm)	K_{IC} ksi · $in^{1/2}$ (MPa · $m^{1/2}$)
DCT-1	*1.35 (6.01)*	0.22 (1.51)	0.0075 (0.1905)	7.19 (7.90)
DCT-2	1.69 (7.51)	0.26 (1.82)	0.0046 (0.1174)	5.38 (5.91)
DCT-3	1.21 (5.40)	0.19 (1.32)	0.0074 (0.1886)	5.66 (6.22)
DCT-4	1.00 (4.47)	0.17 (1.16)	0.0067 (0.1698)	5.80 (6.37)
DCT-5	1.50 (6.66)	0.24 (1.66)	0.0106 (0.2687)	8.72 (9.58)
DCT-6	0.98 (4.36)	0.15 (1.07)	0.0059 (0.1499)	5.03 (5.53)
DCT-7	1.25 (5.56)	0.20 (1.40)	0.0064 (0.1621)	7.11 (7.81)
DCT-8	1.15 (5.11)	0.19 (1.30)	0.0061 (0.1542)	5.88 (6.46)
DCT-9	1.20 (5.34)	0.20 (1.36)	0.0087 (0.2218)	7.53 (8.28)
DCT-10	1.29 (5.75)	0.21 (1.47)	0.0107 (0.2707)	7.79 (8.56)
Average	1.26 (5.62)	0.20 (1.41)	0.0075 (0.1894)	6.61 (7.26)
Standard deviation	0.21 (0.95)	0.03 (0.22)	0.0020 (0.0506)	1.22 (1.34)
Coefficient of variation	17%	17%	27%	18%

Table 4. SEN(B) fracture parameters

Specimen	Force kip (kN)	$CTOD_c$ in (mm)	K_{IC} ksi · $in^{1/2}$ (MPa · $m^{1/2}$)
SEN(B)-1	3.02 (13.43)	0.0095 (0.2400)	8.56 (9.41)
SEN(B)-2	2.74 (12.19)	0.0088 (0.2235)	7.60 (8.35)
SEN(B)-3	2.80 (12.46)	0.0051 (0.1284)	5.05 (5.55)
SEN(B)-4	2.76 (12.28)	0.0076 (0.1926)	6.48 (7.12)
SEN(B)-5	2.35 (10.45)	0.0054 (0.1380)	4.96 (5.45)
SEN(B)-6	2.15 (9.56)	0.0093 (0.2355)	5.75 (6.32)
Average	2.64 (11.73)	0.0076 (0.1930)	6.40 (7.03)
Standard deviation	0.32 (1.43)	0.0019 (0.0493)	1.44 (1.59)
Coefficient of variation	12%	26%	23%

Based on Table 5 and Table 6, it can be seen that the tensile strengths of both test methods come to be close, with a tensile strength average of 1.24 ksi (8.56 MPa) for the DEWS specimens and 1.06 ksi (7.32 MPa) for the direct tension beams. It was verified that the averages are statistically identical with a 95% confidence interval for a two-sample t-test. The fact that DEWS specimens had a slightly higher stress average could be explained by a small friction force acting at the interface between the steel rollers and specimen (even with the application of metal assembly paste). The average flexural stress calculated according to ASTM C1609/C1609M from the four-point bending beam tests is 3.14 ksi (21.62 MPa). The calculation for this stress (Equation 9) is based on the assumption that the section at peak load is still not cracked and remains elastic. Further inverse analysis studies will be developed to better correlate stresses obtained from this test method with other tests and geometries presented in this experimental investigation.

Table 5. DEWS tensile strength

Specimen	Tensile strength ksi (MPa)
DEWS-1	1.21 (8.34)
DEWS-2	1.03 (7.1)
DEWS-3	1.4 (9.65)
DEWS-4	1.23 (8.48)
DEWS-5	1.13 (7.79)
DEWS-6	1.61 (11.1)
DEWS-7	1.5 (10.34)
DEWS-8	1.15 (7.93)
DEWS-9	1.33 (9.17)
DEWS-10	1.18 (8.14)
DEWS-11	1.31 (9.03)
DEWS-12	1.13 (7.79)
DEWS-13	1.11 (7.65)
DEWS-14	1.36 (9.38)
DEWS-15	0.94 (6.48)
Average	1.24 (8.56)
Standard deviation	0.18 (1.23)
Coefficient of variation	14%

Table 6. Direct tension beam tensile strength

Specimen	Tensile strength ksi (MPa)
DT-1	1.19 (8.23)
DT-2	0.97 (6.69)
DT-3	1.01 (6.96)
DT-4	1.02 (7.06)
DT-5	1.18 (8.16)
DT-6	1.07 (7.40)
DT-7	1.13 (7.79)
DT-8	0.97 (6.72)
DT-9	1.00 (6.90)
Average	1.06 (7.32)
Standard deviation	0.09 (0.60)
Coefficient of variation	8%

Table 7. Four-point bending beam flexural stress

Specimen	Flexural stress ksi (MPa)
4PB-1	3.17 (21.84)
4PB-2	3.09 (21.32)
4PB-3	3.15 (21.72)
4PB-4	2.45 (16.87)
4PB-5	3.91 (26.95)
4PB-6	3.27 (20.13)
4PB-7	2.92 (21.62)
Average	3.14 (21.62)
Standard deviation	0.44 (3.01)
Coefficient of variation	14%

6. Conclusions

Five different test methods are presented to evaluate and correlate fracture parameters of UHPC and tensile stresses. The presented test methods include the DCT test, DEWS test, SEN(B) test, four-point bending test, and direct-tension test. The DCT and SEN(B) fracture parameters K_{IC} and $CTOD_c$ were compared and found to be statistically identical. The benefit of using DCT instead of SEN(B) is the geometry, which can be obtained from laboratory cylinder molds or field cores. Finally, the fracture properties from the DCT or SEN(B) test can be input into a detailed finite element modeling software to obtain a tensile stress-strain behavior for UHPC. The tensile strength of the DEWS specimens and direct tension beams were compared and were also observed to be statistically identical, with a difference of 0.18 ksi (1.24 MPa) between the averages. The advantage of the DEWS geometry is that it can be obtained from circular cores taken from an existing structure, and its test setup requires a compression machine instead of tension equipment, which could potentially reduce the testing cost. Further research needs to be performed to better correlate the five different types of tests presented in this experimental investigation. Future studies

including forward and inverse analysis using finite element modeling software will be implemented, which will allow a better comparison and correlation among all the test types presented.

7. References

ASTM Standard C1609/C1609M, "Standard Test Method for Flexural Performance of Fiber-Reinforced Concrete (Using Beam With Third-Point Loading)", ASTM International, West Conshohocken, PA, 2012, DOI: 10.1520/C1609_C1609M-12, www.astm.org.

ASTM Standard C1856/C1856M, "Standard practice for Fabricating and Testing Specimens of Ultra-High Performance Concrete", ASTM International, West Conshohocken, PA, 2017, DOI: 10.1520/C1856_C1856M-17, www.astm.org.

Amirkhanian, A. N., et al. "Forward and Inverse Analysis of Concrete Fracture Using the Disk-Shaped Compact Tension Test." *Journal of Testing and Evaluation* (2015).

di Prisco, M., L. Ferrara and M. G. L. Lamperti. "Double edge wedge splitting (DEWS): an indirect tension test to identify post-cracking behaviour of fibre reinforced cementitious composites." *Materials and Structures* (2013): 1893-1918.

Graybeal, B. and F. Baby. "Development of Direct Tension Test Method for Ultra-High-Performance Fiber-Reinforced Concrete." *ACI Materials Journal* (2013): 177-185.

Graybeal, B. "UHPC Making Strides." 2009.

—. *Ultra-High Performance Concrete*. McLean: Federal Highway Administration, 2006.

Jenq, Y. and S. P. Shah. "Two Parameter Fracture Model for Concrete." *Journal of Engineering Mechanics* (1985): 1227-1241.

Lorenzo, M., et al. "Composite UHPC-AAC/CLC facade elements with modifiel interior plaster for new buildings and refurbishment. Materials and production technology." *Journal of Facade Design and Engineering* (2015): 91-102.

Perry, V. H. "Ultra-High-Performance-Concrete Advancements and Industrializations." *Advances in Civil Engineering Materials* (2015).

RILEM, "Determination of Fracture Parameters (K_{IC} and $CTOD_c$) of Plain Concrete Using Three-Point Bend Tests", RILEM Committee on Fracture Mechanics of Concrete-Test Methods, *Mater. Struct*., Vol. 23, No. 138, 1990: 457-460.

Sritharan, S. "Design of UHPC Structural Members: Lessons Learned and ASTM Test Requirements." *Advances in Civil Engineering Materials* (2015): 113-131.